




CELLULOSE AND LIGNIN FIBERS MEDIATED REMOVAL OF THE OIL SPILL POLLUTION

Daniel ARGHIROPOL^a, Tiberiu RUSU^a,
Miuța Rafila FILIP^a, Codruța SAROSI^b ,
Laura SILAGHI-DUMITRESCU^b ,
Gertrud-Alexandra PALTINEAN^{b,*} 

ABSTRACT. Vegetal matter like hemp wastes, peat and sawdust have fibrous and porous morphology if they are properly shredded as observed in SEM images. Polarized light microscopy has been used to study the crystalline structure of biomass and FTIR spectroscopy evidences their specific chemical bonds. Hemp wastes reveal porous husk remains of about 50 – 500 μm abundant in lignin and cellulose fibers lint having length of about 5 – 50 μm . Shredded peat reveal finer cellulose fibrous formation of about 50 μm length and lignin shell like particles of about 20 – 200 μm . Saw dust contains mainly cellulose fibers grouped in flake particles of about 700 μm with fringed edges. These samples were subjected to diesel and oil spills. The gravimetric test indicates the best specific absorption for diesel of 1.76 g/g obtained by sawdust and the lower value of 1.48 g/g was measured for hemp waste. The oil spill was better absorbed by sawdust having a specific absorption of 2.28 g/g and the weaker absorption was measured for hemp wastes around 1.66 g/g. The lower values measured for peat are caused by the presence of quartz particles as forest soil impurity.

Keywords: *Petroleum hydrocarbons, vegetal absorbents, Cellulose fibers.*

^a Faculty of Materials and Environmental Engineering, Technical University of Cluj-Napoca, 400641 Cluj-Napoca, Romania.

^b Babeș-Bolyai University, “Raluca Ripan” Institute for Research in Chemistry, 30 Fântânele Str., 400294 Cluj-Napoca, Romania.

* Corresponding author: gertrud.paltinean@ubbcluj.ro



INTRODUCTION

Petroleum hydrocarbon pollution poses a significant risk to both the environment and human health. They are hazardous chemicals from various activities such as petroleum industry, vehicle traffic, oil drilling processes, accidental spills, volcanic eruptions [1-3]. Petroleum, gasoline and diesel are the most used fuels which can lead to a significant release of hydrocarbons in aquatic and terrestrial ecosystem. Their infiltration in environment can generate considerable damages such as loss of biodiversity, fertility and productivity [4-7].

To mitigate its harmful effects, natural absorbents have been employed to help restore balance to affected ecosystems. Hydrocarbon absorption is a fast, straightforward, and broadly applicable technique that uses materials capable of capturing and holding pollutants to lessen environmental impact. These absorbents are gaining attention due to their affordability, biodegradability, high oil absorption capacity, high buoyancy, local availability, and low cost [8, 9]. The decontamination of petroleum hydrocarbons using sawdust, peat and hemp fibers as absorbents proved to be beneficial to the environment [10-12].

Wood sawdust is commonly used in the treatment of oil-contaminated water. Its effectiveness varies depending on the type of wood as well as particle size and moisture content. Sawdust is an efficient absorbent due to its porous structure and the presence of carboxyl and hydroxyl functional groups that allows it to capture both volatile and semi-volatile hydrocarbon fractions [13, 14].

Peat is a natural absorbent composed of lignin, cellulose, as well as fulvic and humic acids. Its porous structure offers a large surface area, giving it a high capacity for hydrocarbon absorption. Peat is also highly buoyant and minimizes the risk of secondary pollution during the recovery process [15].

Taking into consideration the actual state regarding the vegetal absorbents used for the oil spills removal, the aim of present article is to evaluate the viability of hemp wastes, shredded peat and sawdust. All these materials are rich in cellulose and lignin having a great potential to be used as absorbents for petroleum wastes.

RESULTS AND DISCUSSION

Vegetal absorbents are known for their textured morphology, which can be properly observed under Scanning Electron Microscopy (SEM). The series of vegetal samples begins with the shredded hemp waste, Figure 1a.

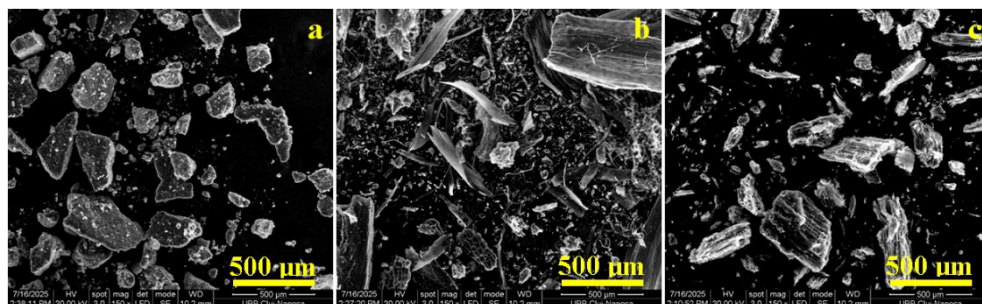


Figure 1. SEM images of the vegetal absorbents samples:
a) Shredded hemp waste, b) Shredded peat and c) Wood sawdust.

This mainly highlights husks from seeds that have a bimodal component formed by the fine fractions predominantly below 20 µm surrounding the coarse fractions that have irregular edges and planar dimensions of 100 – 700 µm associated with a thickness of about 30 – 50 µm.

On the other hand, the shredded peat sample, Figure 1b, contains partially degraded plant material in a wet state, which favors the loosening of the cellulose fibers from the lignified matrix, forming very fine filiform structures with lengths of 500 – 800 µm and thickness of 20 – 50 µm. These surround larger pieces with a still predominantly lignin aspect that gives them cohesion and resistance. We mention that the peat was ground for 30 minutes at 6000 rpm using a blade mill.

The wood sawdust, Figure 1c, is clearly inferior to the peat sample because the cellulose fibers are still strongly bound in the lignified structure, which leads to the predominance of coarse fractions with a chopped appearance (500 – 900 µm) and too few fine fractions to ensure efficient absorption.

Vegetal samples are very abundant in amorphous organic matter which cannot be observed properly in the mineralogical optical microscopy (MOM) but their cohesion is ensured by cellulose fibers and lignin binders which are organic matter with lower crystallinity [15, 16]. Therefore, some of our previous study successfully identifies cellulose fibers having white – yellow appearance and lignin structures predominantly brown under cross polarized light [17, 18]. Thus, the vegetal samples aspect is displayed in Figure 2.

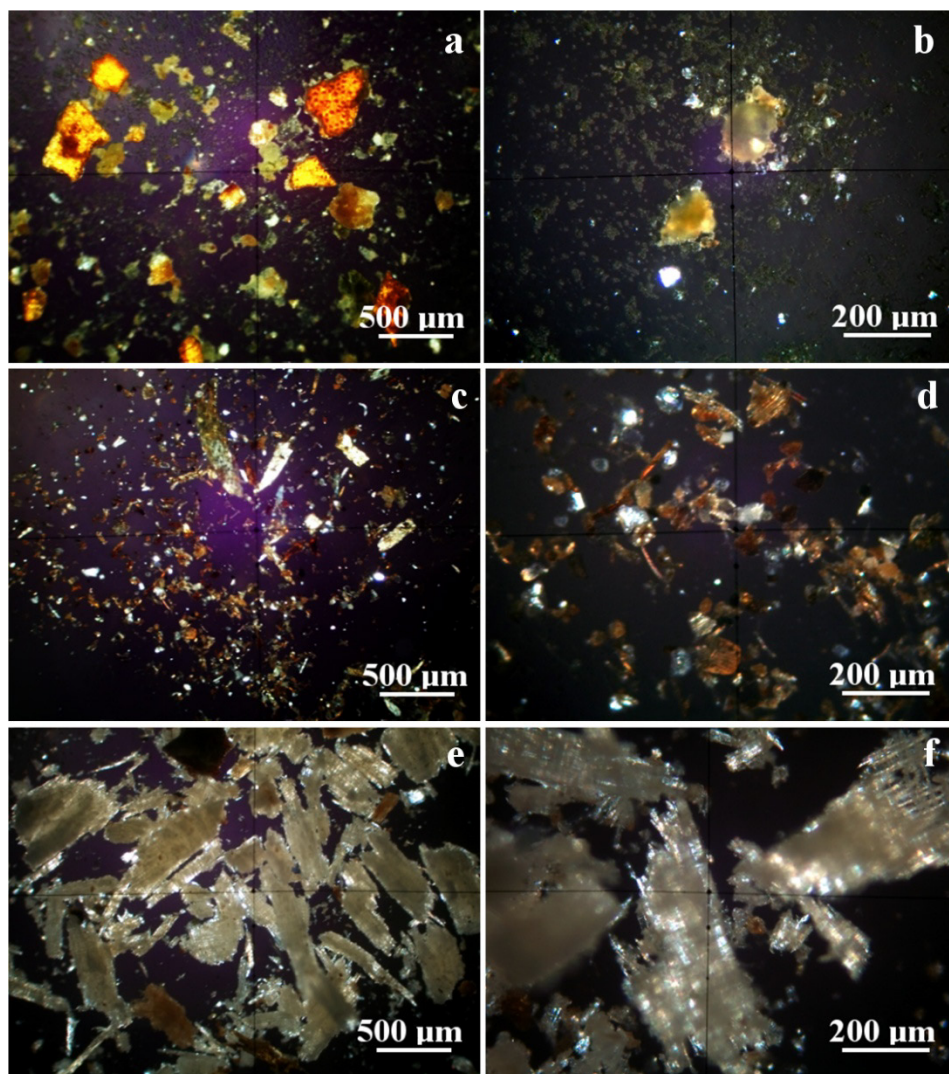


Figure 2. Cross polarized light images of the vegetal absorbents samples:
Shredded hemp waste a) overall appearance, b) microstructural detail;
Shredded peat c) overall appearance, d) microstructural detail; Sawdust
e) overall appearance, f) microstructural detail.

Hemp waste is often a difficult material to naturally biodegrade due to its fibrous texture. The tow can be used as filler such as in the void space between building panels or as a protective coating over certain pipes, but the powdery fractions associated with hemp waste are quite problematic. These,

being ground to a uniform consistency, could act optimally to absorb oil stains. The overall microstructure, Figure 2a, highlights two major components, namely remnants of the husk that covers the hemp fibers. They have a predominantly reddish-brown appearance due to the high lignin content in their structure, which indicates that the stems were harvested at maturity. Their shape is irregular - fringed with planar dimensions varying widely in the range of 50 - 500 μm and the thickness varies between 1 - 5 μm . On the surface of larger shell fragments, circular cell holes with diameters ranging from 5 - 10 μm are observed. These biological reminiscences can be of great use in the absorption and immobilization of petroleum waste due to their high viscosity, which facilitates the retention of liquid in the cell pores.

The second major component of the shredded hemp sample is formed by fine microscopic fiber lint, a fact supported by their cellulose-based composition that appears yellowish white when observed in polarized light with crossed nicols, a fact consistent with data in the literature [17, 18]. The microscopic detail in Figure 2b captures in the central part of the field of view two fragments of hemp husk surrounded by enlarged fiber lint. These have very small dimensions with lengths ranging between 5 – 25 μm and thicknesses ranging between 1 – 3 μm . Their high number correlated with the porous appearance of the husk fragments indicates a high potential for absorption of petroleum waste and oily materials.

Peat has a deep layer with a high degree of carbonization compared to the superficial layers that retain a more pronounced vegetal character [19, 20]. Data from the literature show a significant content of lignin [21] and cellulose [22] of vegetal nature that has not been carbonized. Therefore, it is not surprising that the overall microstructural appearance of the crushed peat sample contains fragments of brown-brown colored lignin and yellowish-white colored cellulose that have a fringed appearance. These are accompanied by compact material particles with a high crystalline character whose nature cannot be detected at such a low magnification as in Figure 2c. The microstructural detail in Figure 2d solves the enigma of mineral particles. These have a boulder-like appearance with rounded edges and the shade is predominantly greenish-gray corresponding to quartz. In fact, these are forest sand particles whose sizes vary in the range of 50 - 100 μm and which are neutral in terms of the absorbing effect (in other words they do not help but do not hinder the absorption process). The particles containing lignin have the appearance of shredded vegetable shells that still retain traces of fibers, the dimensions of these shells vary widely from about 20 μm to 200 μm while the cellulose fibers are rarer and have smaller dimensions, lengths of about 5 - 50 μm and thicknesses of about 5 - 10 μm . Overall, it can be appreciated that such a mixture has a relatively limited ability to absorb petroleum waste due to the large and poorly shredded wood fractions.

Sawdust has an overall appearance of elongated flakes having about 500 – 700 μm length and 50 – 250 μm width. Their color under cross polarized light is white – yellow due to the dense structure of cellulose fibers and contains moderate amount of brown particles rich in lignin, Figure 2e. Some smaller wood dust particles below 20 μm are also observed surrounding the flakes formations. The microstructural detail in Figure 2f reveal that the flakes formation has their ends featuring a fringe network of crossed cellulose fibers generating meshes below 10 μm which are optimal for the viscous liquid absorption. The microstructural disposal of sawdust cellulose fiber is more proactive than occurs in peat sample making it a better candidate for petroleum absorption.

The gravimetric measurements of diesel and burnt engine oil allow us to calculate each material's specific absorption, Figure 3. The obtained results were analyzed statistically and two relevant groups were found.

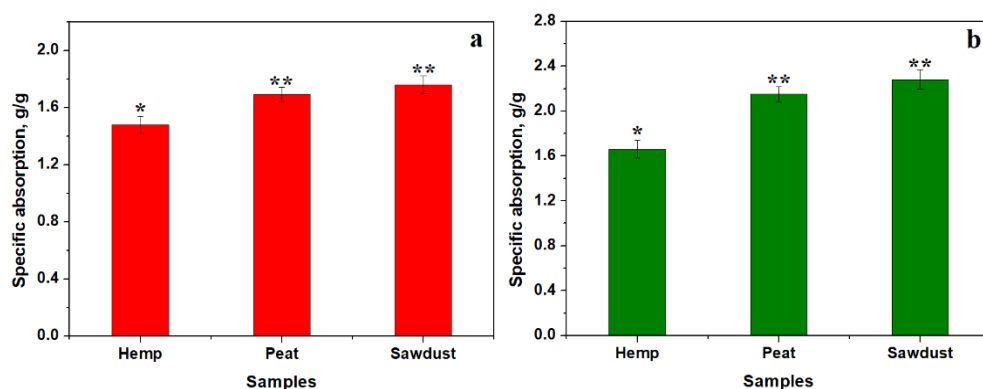


Figure 3. Specific adsorption variation on the vegetal samples tested in: a) Diesel and b) Burnt oil.

At the first sight a major difference is observed between Diesel and burnt oil absorption. The first one is more volatile and therefore the weight uptake is smaller than the one observed for burnt oil within each tested material but the variation tendency is the same in both cases.

The first statistical relevant group is formed by hemp waste sample which ensure a lower specific absorption of both diesel and burnt oil. The second relevant statistical group is formed by the peat and sawdust samples which reveal almost similar specific absorption (peat values being slightly lower). It is perfectly explainable because the wooden fibers within peat samples are partly decayed due to the marsh conditions of the resting ground. The statistical analysis reveals a relevant difference between the identified groups

$p < 0.05$. There must be some microstructural aspect that compromises the hemp waste absorption ability. SEM images taken after absorption, Figure 4, bring light on this aspect.

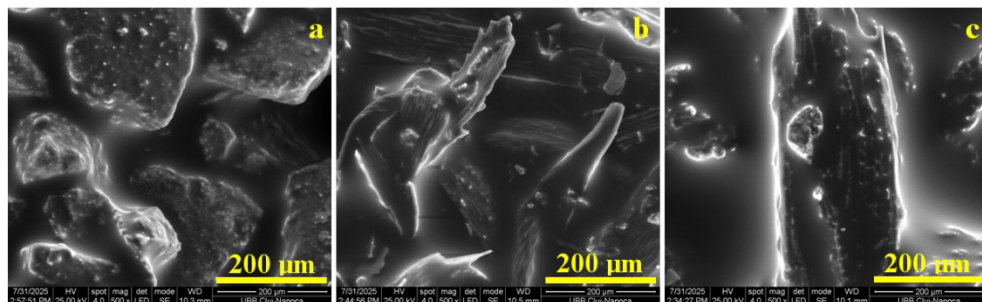


Figure 4. SEM images of the vegetal absorbents after burnt oil absorption: a) Shredded hemp waste, b) Shredded peat and c) Wood sawdust.

Hemp wastes are very abundant in porous crust formations as observed by both initial SEM and cross polarized light microscopy which were taught to be ideal for absorption. Figure 4a, taken after burnt oil absorption reveal the fast penetration of the oil into the shell - crust pores saturating the bigger particles while the fine microscopic cellulose fiber lint is quickly clogged with oil and loses their individualization ability and become stacked to the shell crusts forming a partly barrier in further absorption. Such obstruction was observed in literature by finest mineral particles onto the vegetal particles within the carwash slurry and particulate matter deposits [23, 24]. Thus, the mechanism fails to reach the best absorption. Perhaps the absorption would be increased if the cellulose fiber lint would have been much more numerous than in the present sample.

The fringed cellulose particles within peat sample, Figure 4b, are prone to absorb the burnt oil into their porous structure becoming soaked reaching their optimal load. Their inter-particle space is filled with a dense pellicle of oil increasing the loaded amount. Figure 4c reveal that the fringed structure of sawdust flake particles is more efficient in absorbing petroleum because of their stable meshes network which progressively fill with viscous oil reaching the saturation. The flake particles surface after complete soaking still contains a thicker oil film that stack on the large quantity of absorbed petroleum.

FTIR spectra (Figure 5 and 6) reveals the specific absorption bands for cellulose, lignin and some bands corresponding to hydrocarbons (diesel and burnt oil) in all samples: strong broad OH stretching ($3300\text{--}4000\text{ cm}^{-1}$), C-H stretching in methyl and methylene groups ($2800\text{--}3000\text{ cm}^{-1}$), and a strong broad superposition with sharp and discrete absorptions in the region

from 1000 to 1750 cm^{-1} [25]. The absorption located at $\sim 1730 \text{ cm}^{-1}$ is caused by cellulose and indicates the C=O stretch in non-conjugated ketones, carbonyls and in ester groups [26, 27].

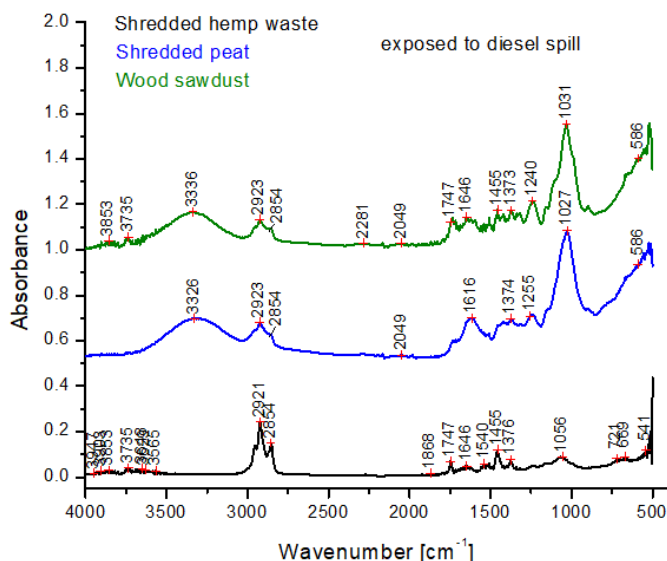


Figure 5. FTIR spectra for vegetal samples exposed to diesel spill.

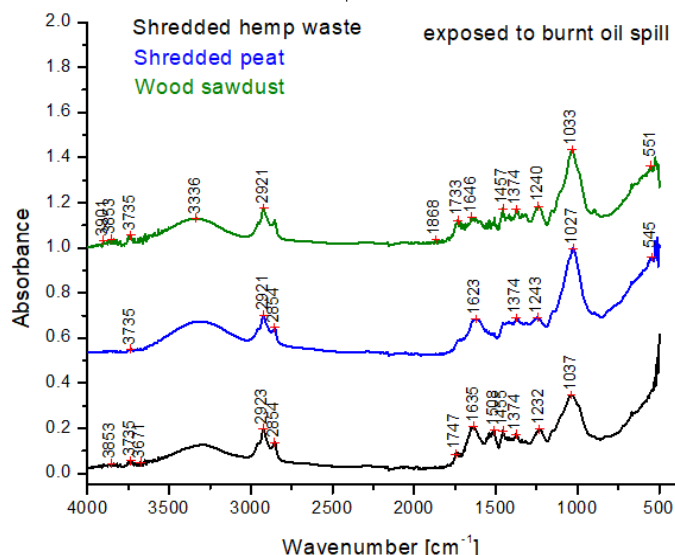


Figure 6. FTIR spectra for vegetal samples exposed to burnt oil spill.

FTIR patterns for peat samples soaked in both diesel and burnt oil reveal absorption bands at 545 cm^{-1} corresponding to O-Si-O bending deformation and 1033 cm^{-1} belonging to the in-plane Si-O stretching within the observed quartz particles [28] that impure the vegetal matter within peat. The other vegetal samples are free of silicates absorption bands.

Band assignments according to the literature and band shifts are listed in Table 1 [25-28].

Table 1. FTIR absorbance bands in vegetable samples (Shredded hemp waste, Shredded peat, Wood sawdust) [25-28].

Wavenumber [cm^{-1}]	Assignment/functional group
3700–3100	O–H stretching vibrations
3000–2750	Symmetric and asymmetric C–H stretching vibrations in CH, CH ₂ , and CH ₃ groups
1770–1700	C=O stretching vibrations in carbonyl and carboxyl groups; C=O stretching vibrations in acetyl fragments
1675–1620	C=O stretching vibrations in <i>p</i> -substituted aromatic ketones
1470–1460	Asymmetric C–H bending vibrations in CH ₂ and CH ₃ groups; Scissor symmetric C–H bending vibrations in CH ₂ groups
1450–1400	C–C stretching skeletal vibrations of the aromatic ring, combined with asymmetric C–H in-plane bending vibrations in O-CH ₃ groups
1380–1370	C–H and O–H bending vibrations
1335–1200	C–H bending vibrations; deformation fan vibrations C–H in CH ₂ groups; O–H in-plane bending vibrations
1145–1000	C–H in-plane bending vibrations of the sugar's rings; C–O stretching vibrations in alcohol groups; symmetric and asymmetric C–O–C stretching vibrations;
545	O-Si-O bending deformation;

A limitation of this study lies in the use of vegetable absorbent materials without any specialized pre-treatment. Future research should focus on investigating how the degree of grinding of the raw materials affects absorbency, aiming to identify optimal processing conditions. The current results clearly show that hemp waste exhibits lower absorption capacity due to its suboptimal microstructural properties. However, with more advanced grinding, these properties could be improved, potentially enhancing the absorption capacity to the level anticipated based on initial microstructural evaluations.

Additionally, further grinding of peat and sawdust samples may also lead to increased specific absorbency. Therefore, subsequent studies should emphasize precise control over the grinding process and incorporate a detailed assessment of porosity, including quantitative analysis of specific surface area using BET (Brunauer–Emmett–Teller) measurements.

CONCLUSIONS

The vegetal absorbents are lighter and therefore float on the water surface making them ideal for decontamination of petroleum spills within the aquatic environment. The best absorption was achieved by sawdust followed closely by peat sample. Hemp waste was slightly ineffective due to rapid clogging of the porous structure within the shell-crusts and the lack of significant network of cellulose fibers.

The microstructural aspects reveal that peat and sawdust have fringed structure of cellulose fibers that ensure an optimal absorption of the petroleum spills (e.g. diesel and burnt oil). Lignin rich parts such lignified crusts are less absorbent and diminish significantly the absorption yield.

Thus FTIR-ATR spectroscopy combined with SEM microscopy models offers a technologic tool that can be applied to evaluated the cellulose and lignin fiber's structure used in mediated removal of the oil spill pollution.

EXPERIMENTAL SECTION

The morphology of the samples, both in their initial state and after absorption, was examined using Scanning Electron Microscopy (SEM) with an Inspect S microscope (FEI Company, Hillsboro, OR, USA), operated in low vacuum mode at an acceleration voltage of 30 kV.

Cellulose and lignin components of the samples were examined under cross-polarized light using a Laboval 2 microscope (Carl Zeiss, Oberkochen, Germany). Each powder sample was carefully spread on a glass slide to ensure optimal visualization. Images were digitally captured using a Samsung 10 MPx camera system.

The quantitative absorption experiment was conducted by weighing 100 grams of each vegetal absorbent powder sample, which was then evenly spread over the contaminated surface. The samples were left in contact with the pollutant for 30 minutes, after which they were collected and reweighed. Specific absorption was calculated by relating the post-decontamination weight to the initial absorbent weight, and expressed as grams of petroleum pollutant absorbed per gram of absorbent. Each experiment was performed in triplicate, with standard deviations represented as error bars in the corresponding graphs. Statistical analysis was carried out using ANOVA followed by Tukey's post hoc test at a significance level of 0.05. Data analysis was performed using Microcal Origin Lab software, version 2018b (Microcal Company, Northampton, MA, USA).

Fourier Transform Infrared Spectroscopy (FTIR) was performed using a JASCO 610 spectrophotometer (JASCO International Co., Ltd., Tokyo, Japan) in ATR mode, with a resolution of 4 cm⁻¹ and 100 scans per spectrum.

REFERENCES

1. S. S. Shetty; D. D. S. Harshitha; S. Sonkusare; P. B. Naik; S. N. Kumari; H. Madhyastha. *Heliyon*, **2023**, 9(9), e19496. <https://doi.org/10.1016/j.heliyon.2023.e19496>
2. M. Rusca; T. Rusu; S. E. Avram; D. Prodan; G. A. Paltinean; M. R. Filip; I. Ciotlaus; P. Pascuta; T. A. Rusu; I. Petean. *Atmosphere*, **2023**, 14, 862. <https://doi.org/10.3390/atmos14050862>
3. M. A. Hoaghia; I. Aschilean; V. Babalau-Fuss; A. Becze; O. Cadar; C. Roman; M. Roman; M. Senila; E. Kovacs. *Studia UBB Chemia*, **2021**, 66(2), 95-104. DOI:10.24193/subbchem.2021.2.08
4. N. N. N. Samsuria; W. Z. W. Ismail; M. N. W. M. Nazli; N. A. A. Aziz; A. K. Ghazali. *Water*, **2025**, 17, 1252. <https://doi.org/10.3390/w17091252>
5. E. Lusweti; E. K. Kanda; J. Obando; M. Makokha, *Water Pract. & Technol.*, **2022**, 17(10), 2171–2185. <https://doi.org/10.2166/wpt.2022.104>
6. F. Ahmed and A. N. M. Fakhruddin. *J. Environ. Sci. & Nat. Resour*, **2018**, 11(3), 555811. DOI: 10.19080/IJESNR.2018.11.555811
7. M. Kamranifar; H. Pourzamani; R. Khosravi; G. Ranjbar; K. Ebrahimpour. *Sci. Rep.*, **2025**, 15, 8459. <https://doi.org/10.1038/s41598-025-92512-9>
8. R. Olga; R. Viktor; I. Alexander; S. Zinnur; P. Alexandra. *Procedia Chemistry*, **2015**, 15, 231-236. <https://doi.org/10.1016/j.proche.2015.10.037>
9. M. R. Pires; M. S. Lorenço; M. C. Dias; L. R. da Silva; I. Petri Junior; F. A. Mori. *Chem. Eng. Technol.*, **2021**, 44(12), 2269–2278. <https://doi.org/10.1002/ceat.202100105>
10. D. Zang; F. Liu; M. Zhang; Z. Gao; C. Wang. *Chem. Eng. Res. Des.*, **2015**, 102, 34–41. <https://doi.org/10.1016/j.cherd.2015.06.014>
11. C. Cojocar; M. Macoveanu; I. Cretescu. *Colloids Surf. A: Physicochem. Eng. Asp.*, **2011**, 384, 675–684. doi:10.1016/j.colsurfa.2011.05.036
12. C. Mongioví; N. Morin-Crini; V. Placet; C. Bradu; A. R. Lado Ribeiro; A. Ivanovska; M. Kostić; B. Martel; C. Cosentino; G. Torri; V. Rizzi; J. Gubitosa; P. Fini; P. Cosma; E. Lichtfouse; D. Lacalamita; E. Mesto; E. Schingaro; N. De Vietro; G. Crini. *Hemp-Based Materials for Applications in Wastewater Treatment by Biosorption-Oriented Processes: A Review*. Edited by D. C. Agrawal; R. Kumar; M. Dhanasekaran in *Cannabis/Hemp for Sustainable Agriculture and Materials*, Springer Singapore, **2022**, pp. 239-295.
13. E. Meez; A. Hosseini-Bandegharai; A. Rahdar; A. Thysiadou; K. A. Matis; G. Z. Kyzas. *Biointerface Research in Applied Chemistry*, **2021**, 11(4), 11778 – 11796. <https://doi.org/10.33263/BRIAC114.1177811796>

14. X. Chen; R. Xu; Y. Xu; H. Hu; S. Pan; H. Pan. *J. Hazard. Mater.*, **2018**, 350, 38-45. <https://doi.org/10.1016/j.jhazmat.2018.01.057>
15. L. Di Giorgio, L. Martín, P.R. Salgado, A.N. Mauri, *Carbohydr. Polym.*, **2020**, 238, 116187. <https://doi.org/10.1016/j.carbpol.2020.116187>
16. P.R. Seidl, A.K. Goulart, *Curr. Opin. Green Sustain. Chem.*, **2016**, 2, 48-53. <https://doi.org/10.1016/j.cogsc.2016.09.003>
17. S.E. Avram, L.B. Tudoran, C. Cuc, B. Borodi, B.V. Birle, I. Petean, *J. Compos. Sci.*, **2024**, 8, 542. <https://doi.org/10.3390/jcs8120542>
18. M. Filip, M. Vlassa, I. Petean, I. Țăranu, D. Marin, I. Perhaită, D. Prodan, G. Borodi, C. Dragomir, *Agriculture*, **2024**, 14, 2038. <https://doi.org/10.3390/agriculture14112038>
19. J. Shen, Y. Qin, J. Wang, Y. Shen, G. Wang, *Minerals*, **2018**, 8, 82. <https://doi.org/10.3390/min8030082>
20. H.I. Petersen, S. Lindström, H.P. Nytoft, P. Rosenberg, *Int. J. Coal Geol.*, **2009**, 78, 119-134. <https://doi.org/10.1016/j.coal.2008.11.003>
21. M. Safaei-Farouji, D. Misch, R.F. Sachsenhofer, J. Weitz, I. Kojic, K. Stojanović, S. Tursyngaliyev, M. Junussov, M.; Fustic, *Int. J. Coal Geol.*, **2025**, 306, 104813. <https://doi.org/10.1016/j.coal.2025.104813>
22. A. Zdravkov, A. Bechtel, K. Stojanović, D. Groß, J. Weitz, I. Kojić, R.F. Sachsenhofer, D. Misch, D. Životić, *Int. J. Coal Geol.*, **2025**, 104843, <https://doi.org/10.1016/j.coal.2025.104843>
23. S.E. Avram, L.B. Tudoran, G. Borodi, M.R. Filip, I. Ciotlaus, I. Petean, *Sustainability*, **2025**, 17, 2906. <https://doi.org/10.3390/su17072906>
24. G.A. Păltinean, I. Petean, G. Arghir, D. F. Muntean, L.-D. Boboș, M. Tomoaia-Cotișel, *Part. Sci. Technol.*, **2016**, 34 (5), 580.
25. S.G. Kostryukov, H.B. Matyakubov, Yu. Yu. Masterova, A. Sh. Kozlov, M.K. Pryanichnikova, A.A. Pynenkova, N.A. Khlichina, *J. Anal. Chem.*, **2023**, 78 (6), 718. <https://doi.org/10.1134/S1061934823040093>
26. Y. Wang, J. Xiang, Y. Tang, W. Chen, & Y. Xu, *Appl. Spectrosc. Rev.*, **2021**, 57(4), 300. <https://doi.org/10.1080/05704928.2021.1875481>
27. R. Javier-Astete, J. Jimenez-Davalos, G. Zolla PLoS ONE **2021**, 16(10), e0256559. <https://doi.org/10.1371/journal.pone.0256559>
28. S.E. Avram, L.B. Tudoran, G. Borodi, M.R. Filip, I. Petean, *Sustainability*, **2025**, 17, 2077. <https://doi.org/10.3390/su17052077>